HIGHER ORDER FINITE - DIFFERENCE APPROXIMATIONS IN NUMERICAL WEATHER PREDICTION.

DONALD CHIN

C

HIGHER ORDER FINITE-DIFFERENCE APPROXIMATIONS

IN NUMERICAL WEATHER PREDICTION

* * * * *

Donald Chin

HIGHER ORDER FINITE-DIFFERENCE APPROXIMATIONS IN NUMERICAL WEATHER PREDICTION

by

Donald Chin
Lieutenant Commander, United States Navy

Submitted in partial fulfillment of
the requirements for the degree of

MASTER OF SCIENCE
IN
METEOROLOGY

United States Naval Postgraduate School
Monterey, California

1 9 6 4

HIGHER ORDER FINITE-DIFFERENCE APPROXIMATIONS

IN NUMERICAL WEATHER PREDICTION

by

Donald Chin

This work is accepted as fulfilling

the thesis requirements for the degree of

MASTER OF SCIENCE

IN

METEOROLOGY

from the

United States Postgraduate School

ABSTRACT

One method of reducing truncation error in numerical prediction is the use of more accurate finite-difference approximations. A relatively simple barotropic model, similar to the one currently in use by the Fleet Numerical Weather Facility (FNWF), Monterey, California, is employed as a basic program in testing several higher order finite-differencing schemes. Forecasts were computed to 24 and 48 hours with modifications of the basic model, and comparisons were made with the analyses at verifying time. It is the intent of this study to determine the effects of some higher order finite-difference approximations in this numerical prediction model.

The author expresses his appreciation to Professor George J. Haltiner for his suggestions, guidance, and patience. Appreciation is also expressed to the personnel of FNWF for providing data and programming assistance.

TABLE OF CONTENTS

TABLE OF SYMBOLS

B	-	tuning constant
C	-	tuning constant
H	-	thickness parameter
P	-	pillow
RMSE	-	root mean square error
Z	-	500-mb height
d	-	grid distance
Δt	-	time interval
η	-	absolute vorticity
ϕ	-	dummy variable
ψ	-	dummy variable
∇^2	-	the Laplacian operator $\nabla^2 = \frac{\partial^2}{\partial x^2} + \frac{\partial^2}{\partial y^2}$
$\mathcal{J}$	-	the Jacobian operator $\mathcal{J}(\phi, \psi) = \frac{\partial \phi}{\partial x}\frac{\partial \psi}{\partial y} - \frac{\partial \phi}{\partial y}\frac{\partial \psi}{\partial x}$

SUBSCRIPTS

a	-	analysis
p	-	predicted
t	-	time
Δt	-	time interval

I. Introduction.

In any numerical method of weather prediction, regardless of the simplicity or complexity of the forecast model, one source of error which cannot be entirely eliminated is the so-called truncation error. This error is mathematical in nature and stems from the use of finite-difference approximations to the derivatives of functions such as those encountered in meteorology. Thompson [7] discusses the problem of truncation error and outlines two methods of reducing the magnitude of the error. The first method involves decreasing the grid interval thereby increasing the number of grid points for a given area. This procedure is not considered in this study. The second method utilizes the "quasi-analytic" property of the functions dealt with in numerical prediction which implies that the functions and their derivatives vary smoothly. If in reality these functions are analytic, uniformly convergent Taylor series can be written for any such functions. The inclusion of higher order terms of the Taylor expansion results in more accurate finite-difference approximations.

It is the purpose of this study to determine the effects of some higher order finite-difference approximations in numerical weather prediction with the intention of obtaining a more accurate prognostication.

2. The Basic Model

The basic model used in this study is a simple model described by Haltiner [4] and similar to the 500-mb barotropic-type forecast currently in operational use by the Fleet Numerical Weather Facility (FNWF), Monterey, California [2]. This model was selected because of its relative simplicity, availability of data in a convenient form, and suitability in programming. It was supposed that a simple model would lend itself best to this type of study. In this model, three empirical terms are incorporated; (a) a "Helmholtz" term, (b) a "latitudinal" term, and (c) a "temperature" term. Although these terms are reported to be relatively small, they are included because they have been found to improve the results.

The equation programmed for the basic model is of the form:

$$\left(\nabla^2 - B\right)\frac{\partial z}{\partial t} = -C\,\mathbb{J}\left(z, \eta + H\right). \tag{1}$$

Equation (1) is solved numerically by a sequential relaxation method. The input parameters are the 500-mb analysis and the thickness of the layer between 1000 mb and 500 mb, with only the values north of 2N entering into the computations. A forward time step is used initially followed by centered-differences at one-hour intervals. At six-hour intervals, slight smoothing is applied and the

ellipticity criterion imposed, after which a forward time step is again initiated and the process repeated.

The finite-difference approximations programmed in the basic forecast scheme can be found in most texts on numerical methods. Collatz [1] provides a comprehensive list of these formulas. Formulas used in the basic program are the 5-point approximation to the Laplacian

$$\nabla^2 Z_0 \simeq \frac{1}{d^2}\left(Z_1 + Z_2 + Z_3 + Z_4 - 4Z_0\right) \tag{2}$$

and the 5-point approximation to the Jacobian

$$\mathbb{J}\left(\phi_0, \psi_0\right) \simeq \frac{1}{4d^2}\left[\left(\phi_2 - \phi_1\right)\left(\psi_3 - \psi_4\right) - \left(\phi_3 - \phi_4\right)\left(\psi_2 - \psi_1\right)\right] \tag{3}$$

where the numerical subscripts refer to the grid position with the 5-point grid defined as

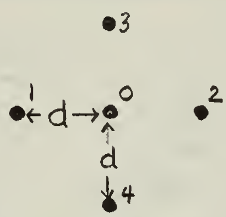

The time stepping formulas consist of the forward-difference

$$Z_{t+\Delta t} = Z_t + \left(\frac{\partial Z}{\partial t}\right)_t \Delta t \tag{4}$$

and the centered-difference

$$Z_{t+\Delta t} = Z_{t-\Delta t} + 2\left(\frac{\partial Z}{\partial t}\right)_t \Delta t \tag{5}$$

where the subscripts refer to the time at which the quantities are computed.

To reduce the truncation error in the basic forecast program many higher order finite-difference formulas are available. Only a few of these formulas are considered in this investigation. To identify the modifications to the basic program, letter designations were given to the changes which are described in the following section.

3. Modification B.

The first modification to the basic program consists of substituting for equation (2) a 9-point approximation to the Laplacian

$$\nabla^2 Z_0 \simeq \frac{1}{4d^2}\left[-60 Z_0 + 16(Z_1+Z_2+Z_3+Z_4) - (Z_5+Z_6+Z_7+Z_8)\right]. \quad (6a)$$

Equation (6a) can also be written symbolically as suggested by Forsythe and Wasow [3]:

$$\nabla^2 Z_0 \simeq \frac{1}{4d^2}\begin{bmatrix} & & -1 & & \\ & & 16 & & \\ -1 & 16 & -60 & 16 & -1 \\ & & 16 & & \\ & & -1 & & \end{bmatrix} Z. \quad (6b)$$

The remainder, representing the residual between the finite-difference approximation and the actual value, consists of sixth-order derivatives and higher.

4. Modification C.

The same grid as presented in section 3 can be used to

derive a 9-point approximation to the Jacobian applying the formula for a 5-point centered-difference along each dimension of the grid. Modification C includes the replacement of equation (3) by

$$J(\phi_0, \psi_0) \simeq \frac{1}{144 d^2}\Big[(\phi_5 - 8\phi_1 + 8\phi_2 - \phi_6)(\psi_8 - 8\psi_4 + 8\psi_3 - \psi_7) - (\phi_8 - 8\phi_4 + 8\phi_3 - \phi_7)(\psi_5 - 8\psi_1 + 8\psi_2 - \psi_6)\Big] \qquad (7)$$

where the subscripts locate the positions on the grid as follows:

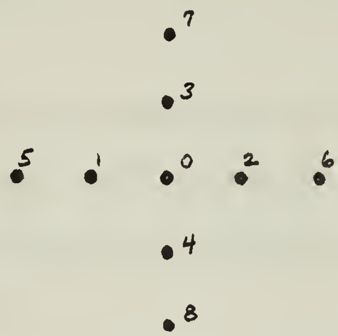

The remainder contains the product of third-order derivatives as the leading term. In both modifications B and C no other changes are made to the basic program, and no additional computer storage space of any significance is required. By the inclusion of both 9-point approximations, equations (6) and (7), a composite program is obtained. This dual program is designated as modification X.

5. Modification D.

In the basic program, equations (4) and (5) are used for the first and second hourly time steps respectively. For this modification, subsequent time steps are performed

by utilizing an approximation comprised of terms through the third derivative as shown:

$$Z_{t+\Delta t} - Z_{t-\Delta t} \simeq 2\left(\frac{\partial Z}{\partial t}\right)_t \Delta t + \frac{2}{3!}\left(\frac{\partial^3 Z}{\partial t^3}\right)_t (\Delta t)^3. \tag{8}$$

By the method of divided differences described by Jennings [5] a formula for equation (8) in terms of Z and $\frac{\partial Z}{\partial t}$ can be derived:

$$Z_{t+\Delta t} = 3\left(\frac{\partial Z}{\partial t}\right)_t \Delta t - \frac{3}{2} Z_t + 3 Z_{t-\Delta t} - \frac{1}{2} Z_{t-2\Delta t}. \tag{9}$$

Equation (9) has the same form as the formula listed in Milne [6] for a net of four equally-spaced points. The remainder can be shown to contain terms higher than the third derivative.

Note that equation (9) contains one additional past point. In programming this modification, one additional field is necessary in the computer memory.

6. Modification E.

Iterations after the first two time steps are accomplished in this case by an alternative method of including the third-order term in equation (8). By considering

$$\frac{\partial^3 Z}{\partial t^3} = \frac{\partial^2}{\partial t^2}\left(\frac{\partial Z}{\partial t}\right)$$

and using a one-sided difference for the second derivative in terms of the first derivative, equation (8) becomes

$$Z_{t+\Delta t} = Z_{t-\Delta t} + \left[\frac{7}{3}\left(\frac{\partial z}{\partial t}\right)_t - \frac{2}{3}\left(\frac{\partial z}{\partial t}\right)_{t-\Delta t} + \frac{1}{3}\left(\frac{\partial z}{\partial t}\right)_{t-2\Delta t} \right]. \tag{10}$$

Equation (10) contains three height-change tendencies and consequently greater computer storage space is required. Due to limited computer storage space and other considerations to be pointed out in section 7, both modifications D and E necessitated considerable revision of the program.

7. Procedures.

All computations were performed with the CDC 1604 all purpose computer using a 63 x 63 square grid with a mesh length of 381 km. The grid is superimposed on a polar stereographic projection of the northern hemisphere centered at the North Pole and true at 60N.

Imput data in the form of 500-mb and 1000-mb analyses on magnetic tape were provided by FNWF. The period from 00Z 15 March 1964 through 00Z 20 March 1964 was used in this study. This period was selected because the synoptic situation showed a block positioned over northern Europe, a series of waves moving rapidly across the Pacific area, and systems developing and weakening across the North American continent. This depicted a variety of conditions for which the programs could be tested.

The prognosis was carried out to 24 and 48 hours for all programs with the exception of modification E. Difficulty was encountered with modification D because of overflow after 36 hours. By a small amount of smoothing at each time step the program was able to operate to no less than 48 hours. Modification E overflowed at 30 hours. Smoothing the height field or the tendency field was ineffective in controlling the instability, hence modification E was terminated at 24 hours.

When each series of computations was completed, the products were compared at each grid point with the analysis at the appropriate verifying times. The pillow and root mean square error were computed for each prognosis. The pillow and root mean square error are denoted respectively:

$$P = \frac{1}{n} \sum_{i=1}^{n} \left(Z_a - Z_p\right)_i$$

and

$$RMSE = \sqrt{\frac{1}{n} \sum_{i=1}^{n} \left[\left(Z_a - Z_p\right)_i - P\right]^2}$$

where n is the number of grid points considered. For this comparison all grid points were used, hence n=3969.

8. Results and Discussion.

The results of the comparisons are given in Table I. It should be noted that the results are slightly biased in favor of the basic program. This is due to the use of the

TABLE I

Pillow and RMSE of verifying analysis and prognosis

Prognosis	Initial Time	24-hr P/RMSE (meters)	48-hr R/RMSE (meters)
Basic	15/00Z	6.4/31.7	7.9/50.3
	16/00Z	2.4/31.1	3.7/54.0
	17/00Z	2.1/35.4	0.3/54.9
	18/00Z	-0.3/29.6	1.8/48.5
Mod B	15/00Z	7.0/47.8	8.2/59.7
	16/00Z	3.1/46.0	5.5/77.8
Mod C	15/00Z	7.6/31.7	9.4/49.1
	16/00Z	3.3/30.5	5.2/52.7
	17/00Z	3.3/34.1	4.7/54.0
	18/00Z	0.3/29.9	3.1/48.1
Mod D	15/00Z	16.8/48.8	44.2/97.6
	16/00Z	12.2/43.3	39.6/86.0
Mod E	15/00Z	8.8/62.2	--
	16/00Z	4.3/55.2	--
Mod X	15/00Z	7.3/50.0	8.8/68.0
	16/00Z	3.1/47.0	5.5/74.0

basic prognosis in the first approximation for producing the verifying analysis. Maps containing the 500-mb height field were printed as a grid for each set of computations and contour charts plotted with the CDC 160 and graph plotter.

The prognoses from 00Z 16 March 1964 for each program, typifying the products obtained, are given in Appendix I. Analyses of the 00Z charts covering the period concerned are also presented.

By examination of the products of the various programs and comparison with the analyses at verifying time, the following observations were made:

(a) All programs show reasonable contour patterns with the exception of modification D. It is obvious from charts 7 and 8 that spurious perturbations with a wavelength on the order of three grid-intervals developed and amplified with time. These waves appear to be caused by computational instability originating from the use of the finite-difference formula.

(b) The major polar low was too deep in all programs, ranging from 20-60 m at 24 hours to 105-160 m at 48 hours. On the other hand, the heights of quasi-stationary systems tended to be too large by an average of 12 m for highs and 70 m for lows at 24 hours, and 43 m for highs and 71 m for lows at 48 hours. The magnitude of the differences tended to contribute to the relative accuracy of the individual programs.

(c) The speed of moving systems was in general slower than the verifying analysis indicated. Interestingly, movements in modifications B and X could hardly be detected in most cases. Recall that modifications B and X both contain

the 9-point approximation to the Laplacian. This change was suspect to possible programming error or incompatibility of the modification and the basic program. A check of the subroutine for the 9-point Laplacian gave reasonable calculations. Consequently, the latter reason is indicated as the cause of the results, especially in view of the tendency for spurious anti-cyclogenesis to creep in. Anti-cyclogenesis was controlled in the other programs.

(d) As expected for barotropic models, all programs suffered when predicting the intensification of developing systems.

Of all the modifications tested, the only one which compares favorably with the basic program is modification C which utilizes the 9-point Jacobian. There is strong evidence that the use of this subroutine can improve the basic program. Due to the limited computer time available, the length of each run (see table II), and other difficulties, a relatively small sample was obtained. Because the 9-point Jacobian program showed more promise, additional data were collected for modification C. Similar data for the basic program were also required to determine if the two methods were comparable. The RMSE for modification C averaged slightly less than the basic program, though the pillow was somewhat higher. There was no significant difference in running time.

TABLE II

Computer running time for the prognoses

Prognosis	24-hr Prog (minutes)	48-hr Prog (minutes)
Basic	12	24
Mod B	14	27
Mod C	12	24
Mod D	24	47
Mod E	27	-
Mod X	16	32

9. Conclusions.

From this investigation, it can be said that although truncation error can be reduced theoretically through the use of higher order finite-differences, the incorporation of these approximations into a numerical prognostication scheme can lead to undesirable effects in some cases. Computational instability and other difficulties encountered in this study point out the implicit complexity of making a seemingly simple change to a forecast method. No modifications other than the substitution of higher order finite-difference formulas were used, except for the small amount of additional smoothing previously mentioned. By adding empirical corrections to the model, it is conceivable that the forecasts could be further improved, but this was

not the primary objective of this paper.

The limited results of this study provide additional avenues of research. One-sided advection schemes and numerous other stencils for the finite-difference approximations are suggested for further examination.

BIBLIOGRAPHY

1. Collatz, L. The numerical treatment of differential equations. Springer, Berlin, 1960.

2. Unpublished notes. Fleet Numerical Weather Facility, Monterey, California, 1963.

3. Forsythe, G. E., and W. R. Wasow. Finite-difference methods for partial differential equations. Wiley and Sons, New York, 1960.

4. Haltiner, G. J. Dynamical analysis of atmospheric waves. Unpublished notes. U. S. Naval Postgraduate School, Monterey, California.

5. Jennings, W. Unpublished notes. U. S. Naval Postgraduate School, Monterey, California, 1963.

6. Milne, W. E. Numerical calculus. Princeton University Press, Princeton, 1949.

7. Thompson, P. D. Numerical weather analysis and prediction. Macmillan Co., New York, 1961.

APPENDIX I

The following charts were produced during this investigation. They are typical of the prognoses obtained by the programs studied. Also included are the analyses of the charts for the period covered.

Charts 1-2	24-hr and 48-hr prognoses, 00Z 16 March 1964 Basic program
Charts 3-4	24-hr and 48-hr prognoses, 00Z 16 March 1964 Modification B
Charts 5-6	24-hr and 48-hr prognoses, 00Z 16 March 1964 Modification C
Charts 7-8	24-hr and 48-hr prognoses, 00Z 16 March 1964 Modification D
Chart 9	24-hr prognoses, 00Z 16 March 1964 Modification E
Charts 10-11	24-hr and 48-hr prognoses, 00Z 16 March 1964 Modification X
Charts 12-17	Analyses, 00Z 15 March 1964 through 00Z 20 March 1964

500 HT 24 HR PROG FROM 00Z 16 MAR 64 CHART 1

PROJECTION: POLAR STEREOGRAPHIC—TRUE AT 60° NORTH LATITUDE
SCALE: 1:60,000,000

FLEET NUMERICAL WEATHER FACILITY
MONTEREY, CALIFORNIA

CHART No. 6-B

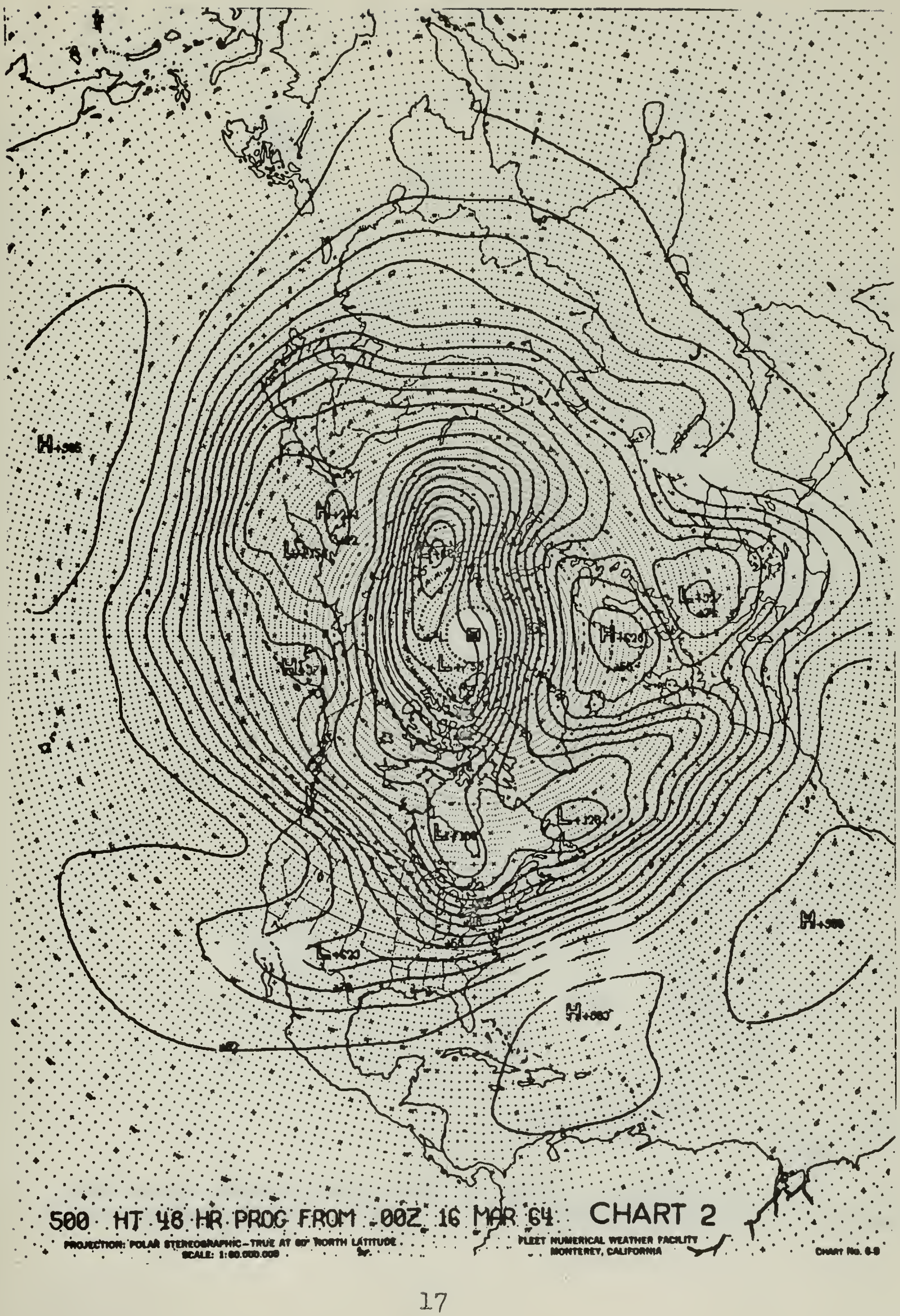
500 HT 48 HR PROG FROM 00Z 16 MAR 64
CHART 2
PROJECTION: POLAR STEREOGRAPHIC—TRUE AT 60° NORTH LATITUDE
FLEET NUMERICAL WEATHER FACILITY
MONTEREY, CALIFORNIA

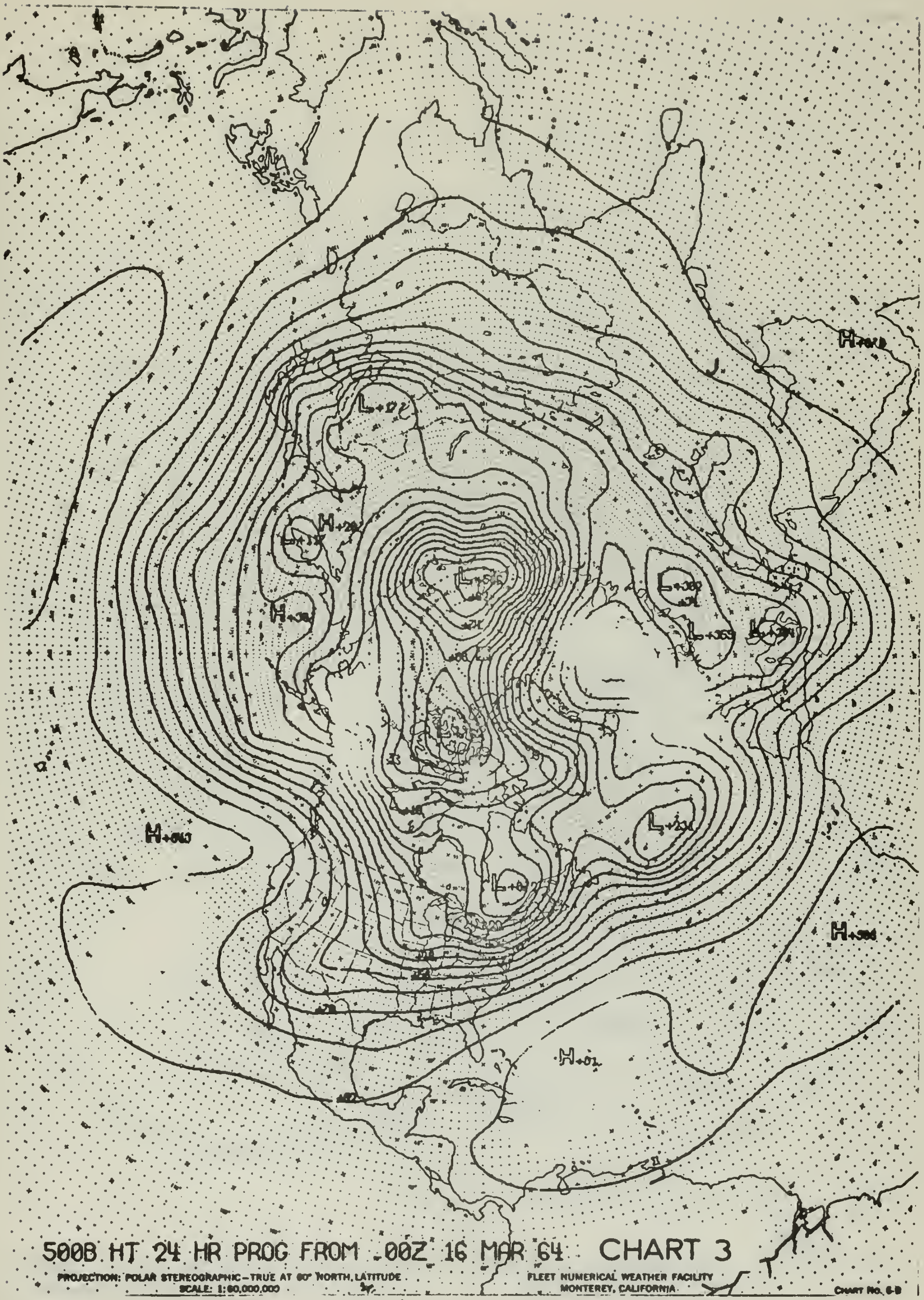

500B HT 24 HR PROG FROM 00Z 16 MAR 64 CHART 3

PROJECTION: POLAR STEREOGRAPHIC—TRUE AT 60° NORTH LATITUDE
SCALE: 1:60,000,000

FLEET NUMERICAL WEATHER FACILITY
MONTEREY, CALIFORNIA

CHART NO. 6-B

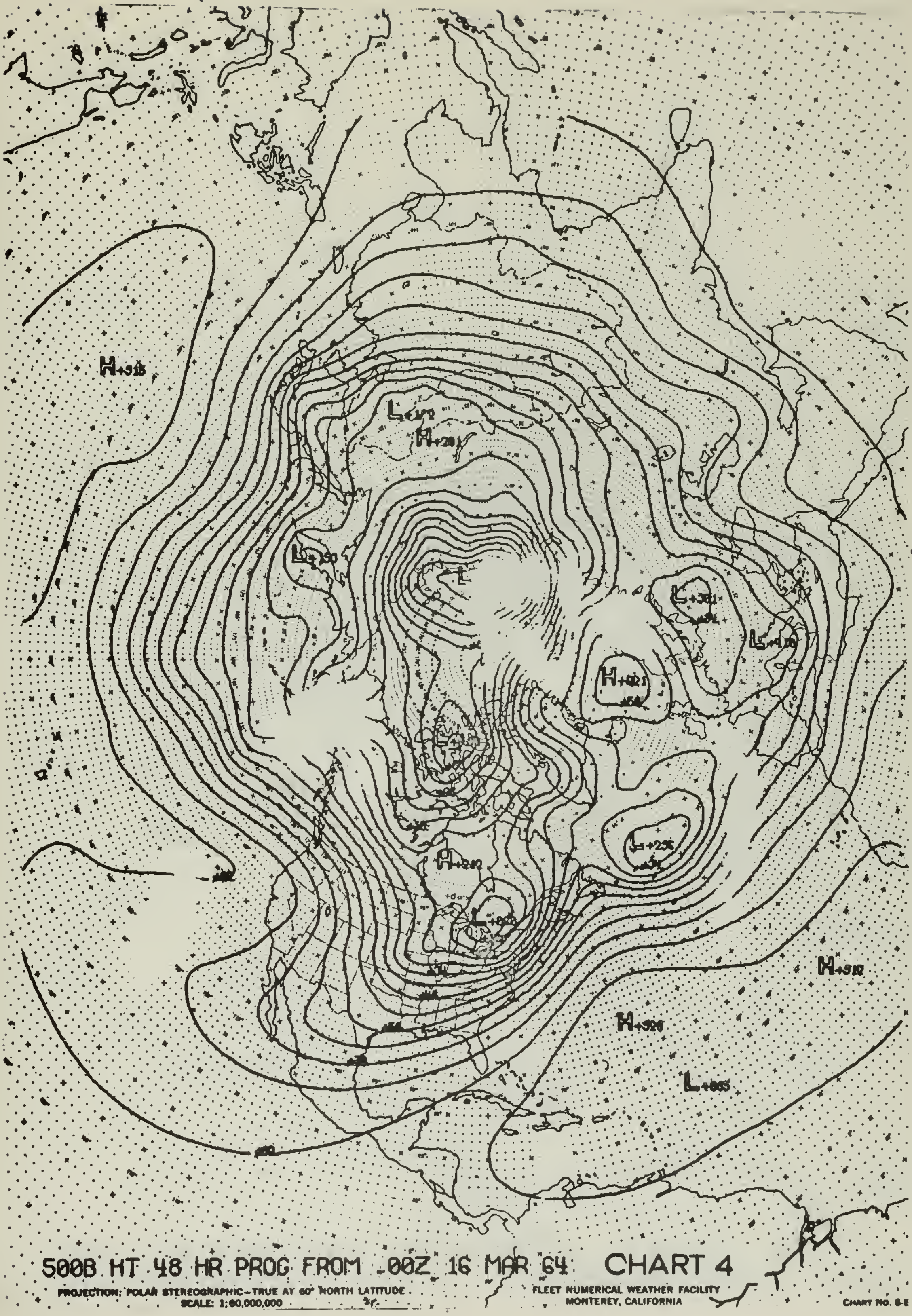
500B HT 48 HR PROG FROM .00Z 16 MAR 64
CHART 4
PROJECTION: POLAR STEREOGRAPHIC—TRUE AT 60° NORTH LATITUDE
SCALE: 1:60,000,000
FLEET NUMERICAL WEATHER FACILITY
MONTEREY, CALIFORNIA

500C HT 24 HR PROG FROM .00Z 16 MAR 64 CHART 5

PROJECTION: POLAR STEREOGRAPHIC—TRUE AT 60° NORTH LATITUDE
SCALE: 1:60,000,000

FLEET NUMERICAL WEATHER FACILITY
MONTEREY, CALIFORNIA

CHART No. 6-B

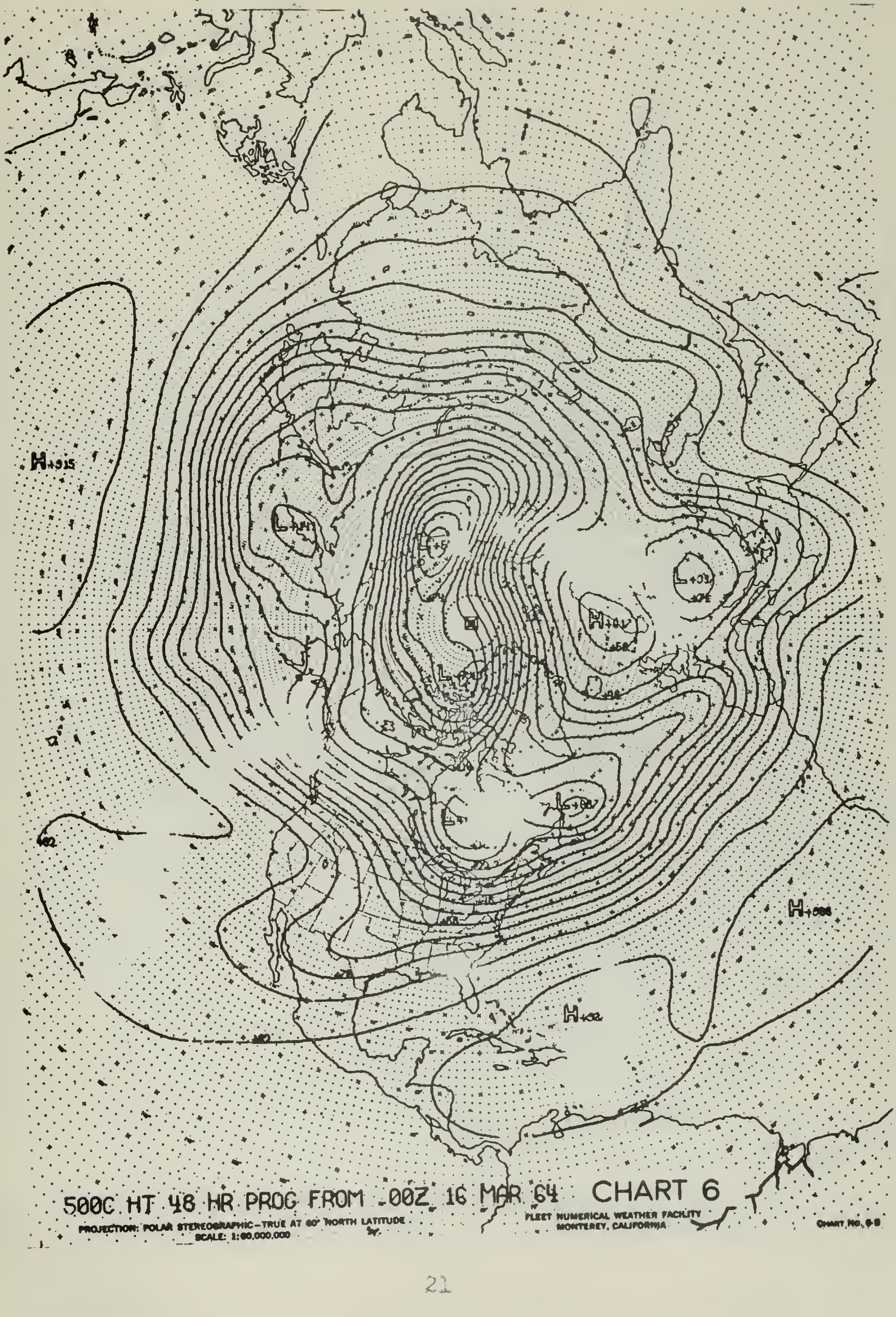
500C HT 48 HR PROG FROM 00Z 16 MAR 64
CHART 6
PROJECTION: POLAR STEREOGRAPHIC—TRUE AT 60° NORTH LATITUDE
SCALE: 1:60,000,000
FLEET NUMERICAL WEATHER FACILITY
MONTEREY, CALIFORNIA

500D HT 24 HR PROG FROM 00Z 16 MAR 64 CHART 7

PROJECTION: POLAR STEREOGRAPHIC—TRUE AT 60° NORTH LATITUDE
SCALE: 1:60,000,000

FLEET NUMERICAL WEATHER FACILITY
MONTEREY, CALIFORNIA

500D HT 48 HR PROG FROM 00Z 16 MAR 64
CHART 8
PROJECTION: POLAR STEREOGRAPHIC—TRUE AT 60° NORTH LATITUDE
SCALE: 1:60,000,000
FLEET NUMERICAL WEATHER FACILITY
MONTEREY, CALIFORNIA


500E HT 24 HR PROG FROM 00Z 16 MAR 64
CHART 9
PROJECTION: POLAR STEREOGRAPHIC—TRUE AT 60° NORTH LATITUDE
SCALE: 1:60,000,000
FLEET NUMERICAL WEATHER FACILITY
MONTEREY, CALIFORNIA

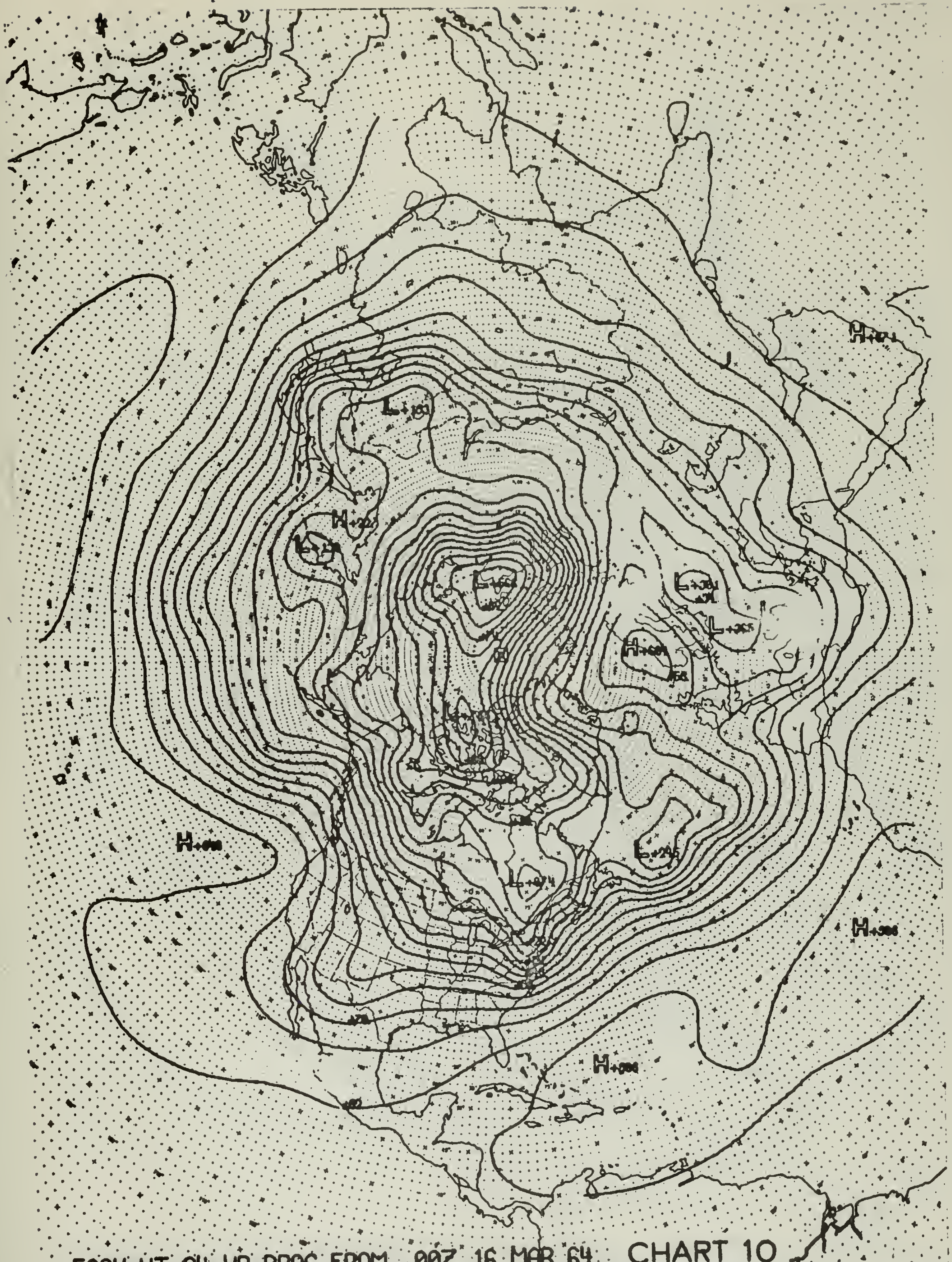
500X HT 24 HR PROG FROM 00Z 16 MAR 64 CHART 10
PROJECTION: POLAR STEREOGRAPHIC—TRUE AT 60° NORTH LATITUDE
SCALE: 1:60,000,000
FLEET NUMERICAL WEATHER FACILITY
MONTEREY, CALIFORNIA

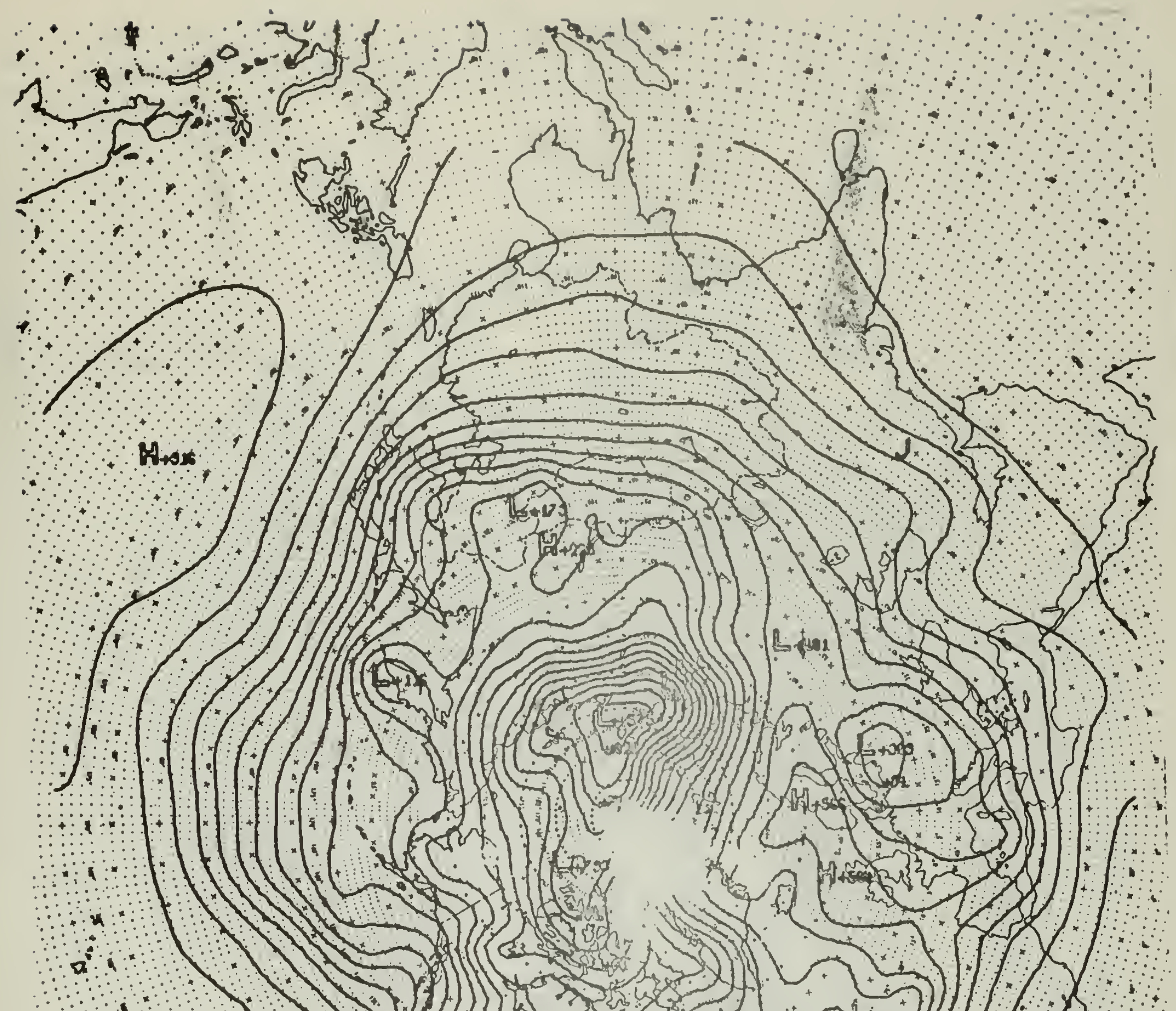

500X HT 48 HR PROG FROM 00Z 16 MAR 64 CHART 11

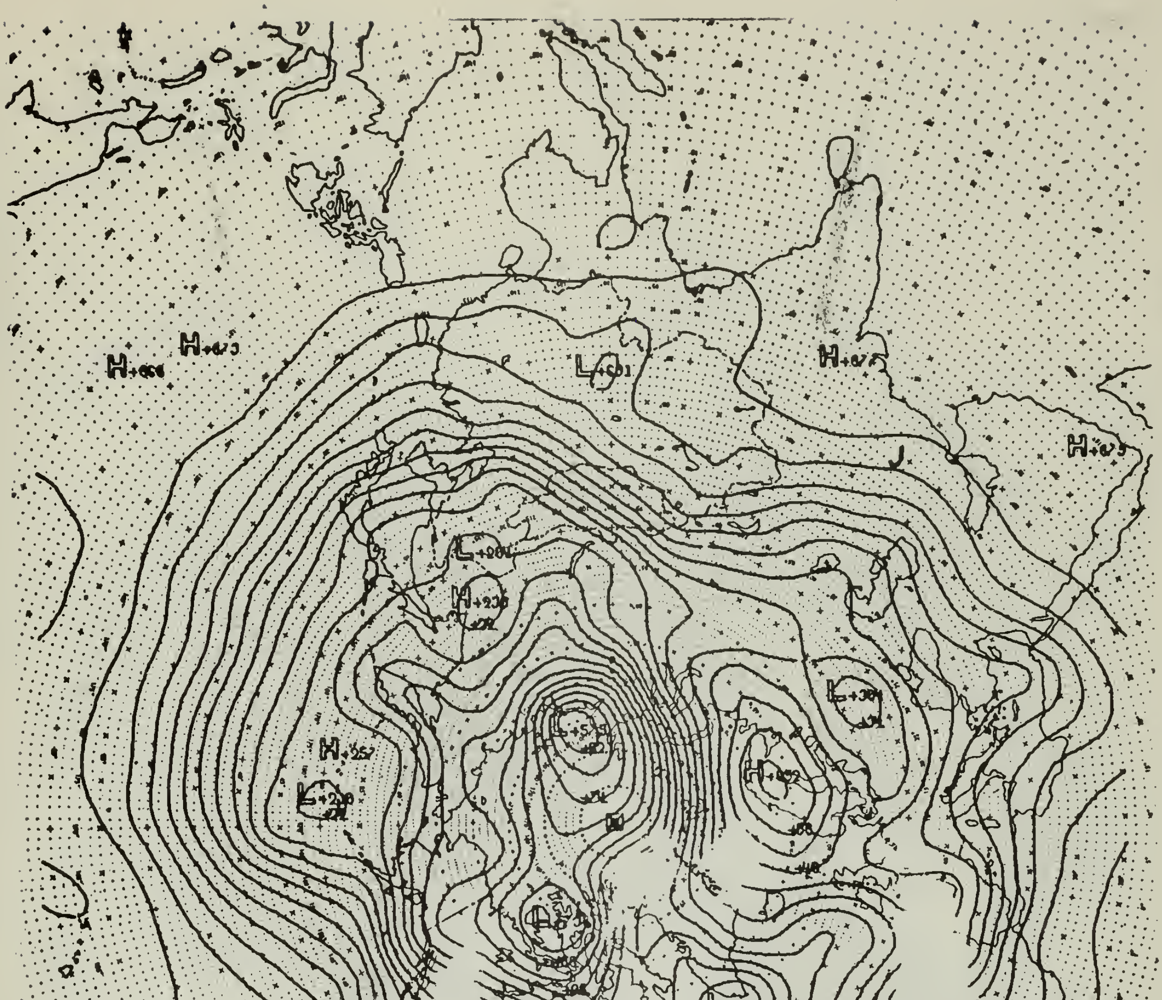
500 HT ANAL 00Z 15 MAR 64
CHART 12
PROJECTION: POLAR STEREOGRAPHIC—TRUE AT 60° NORTH LATITUDE
SCALE: 1:60,000,000
FLEET NUMERICAL WEATHER FACILITY
MONTEREY, CALIFORNIA

500 HT ANAL 00Z 16 MAR 64

CHART 13

PROJECTION: POLAR STEREOGRAPHIC—TRUE AT 60° NORTH LATITUDE
SCALE: 1:60,000,000

FLEET NUMERICAL WEATHER FACILITY
MONTEREY, CALIFORNIA

CHART NO. 6-B


500 HT ANAL 00Z 17 MAR 64
PROJECTION: POLAR STEREOGRAPHIC—TRUE AT 60° NORTH LATITUDE
SCALE: 1:60,000,000
CHART 14
FLEET NUMERICAL WEATHER FACILITY
MONTEREY, CALIFORNIA


500 HT ANAL 00Z 18 MAR 64
PROJECTION: POLAR STEREOGRAPHIC—TRUE AT 60° NORTH LATITUDE
SCALE: 1:60,000,000
CHART 15
FLEET NUMERICAL WEATHER FACILITY
MONTEREY, CALIFORNIA
CHART NO. 6-B

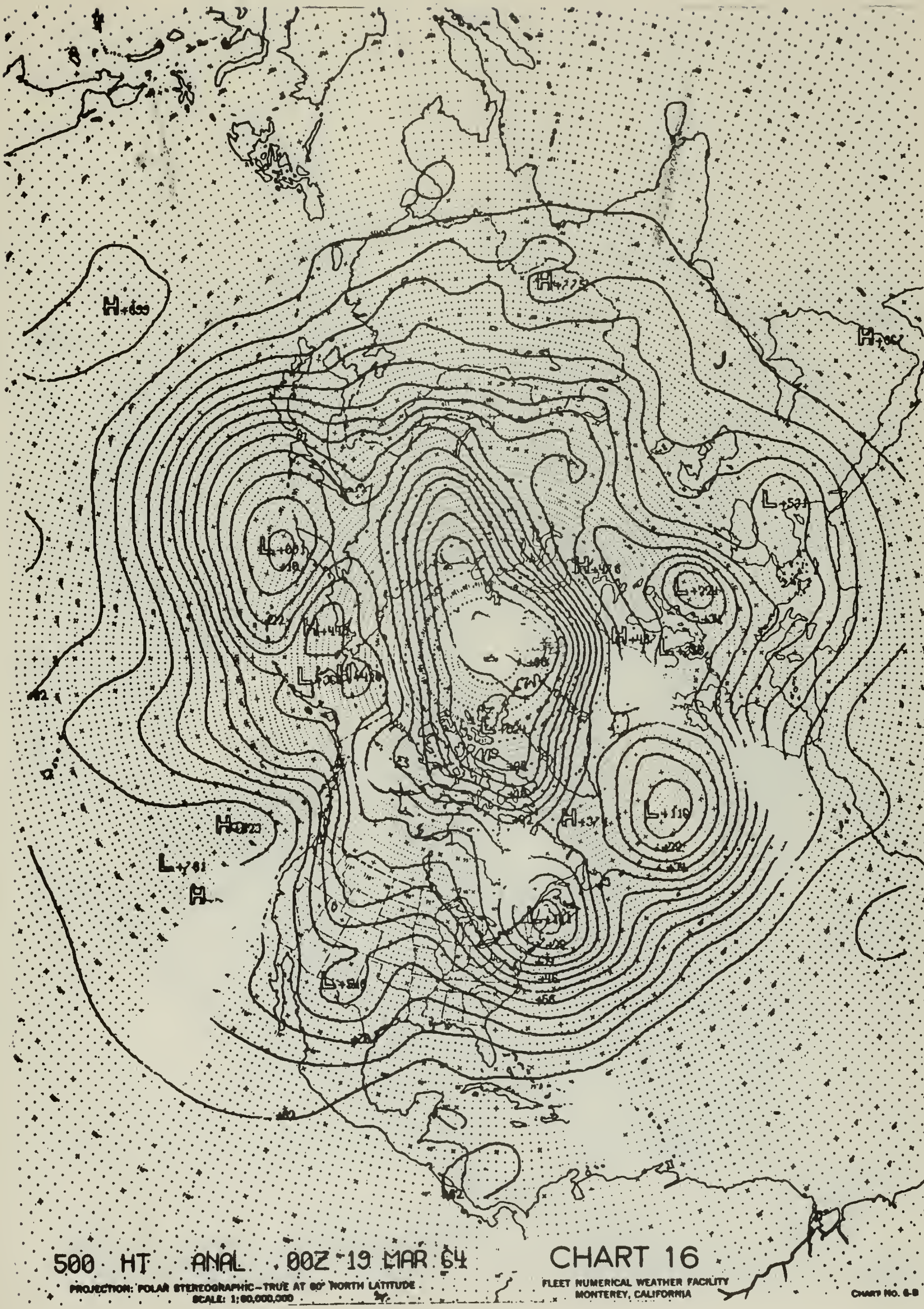

500 HT ANAL 00Z 19 MAR 64
CHART 16
PROJECTION: POLAR STEREOGRAPHIC—TRUE AT 60° NORTH LATITUDE
SCALE: 1:60,000,000
FLEET NUMERICAL WEATHER FACILITY
MONTEREY, CALIFORNIA

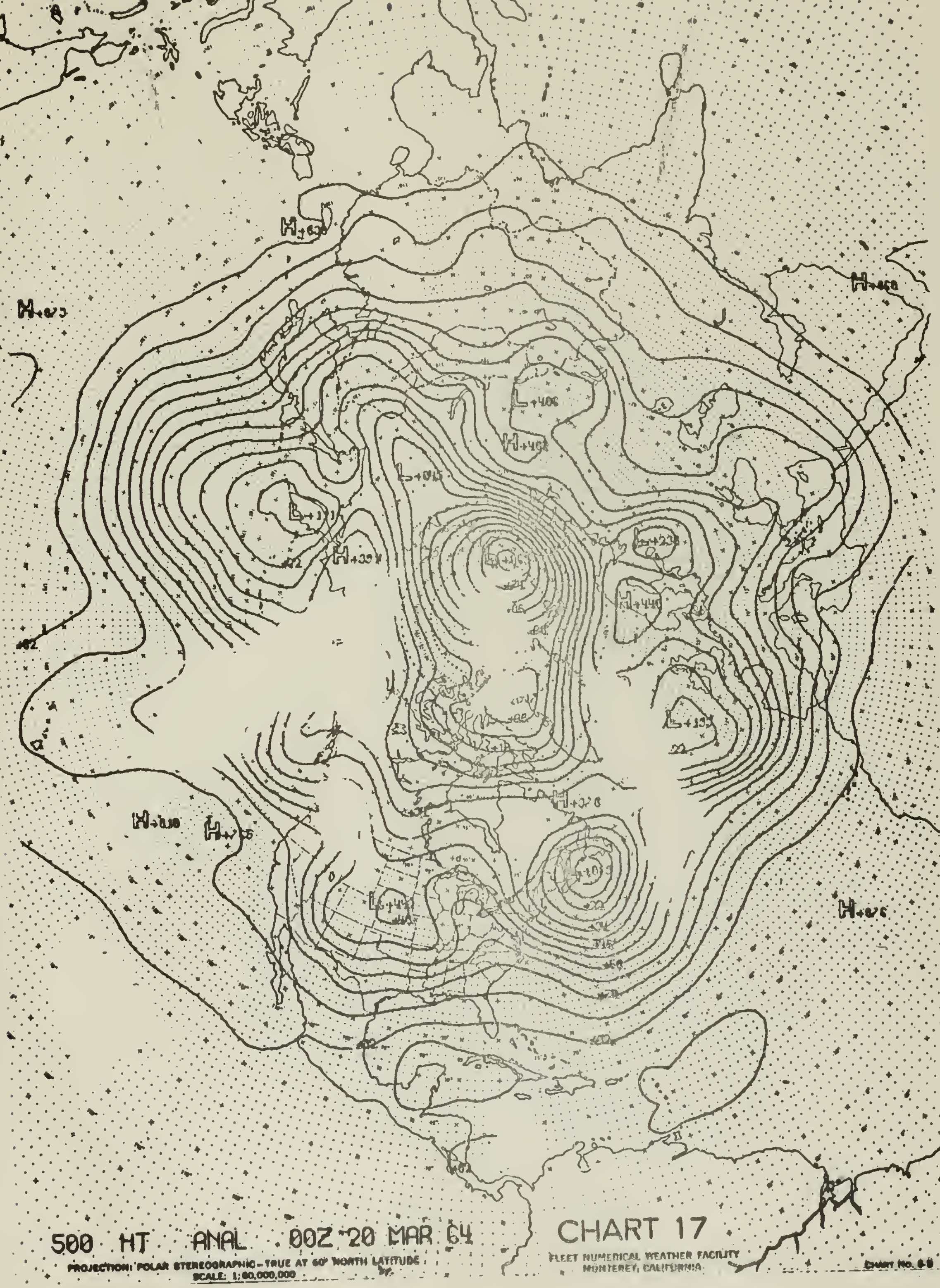

500 HT ANAL 00Z 20 MAR 64

PROJECTION: POLAR STEREOGRAPHIC—TRUE AT 60° NORTH LATITUDE

SCALE: 1:60,000,000

CHART 17

FLEET NUMERICAL WEATHER FACILITY
MONTEREY, CALIFORNIA